

Propane/Diesel Mixed Fuels Spray Angle Investigation in the Near-Nozzle Field via High-Speed Imaging

Ezio Mancaruso, Renato Marialto, Luigi Sequino, Bianca Maria Vaglieco
Istituto Motori – Consiglio Nazionale delle Ricerche, Italy
Luigi Sequino: l.sequino@im.cnr.it

Abstract

The use of fuel blends like diesel/biodiesel, diesel/ethanol, and diesel/gasoline in internal combustion engines is spreading because it can reduce the engine pollutant emissions without significant hardware modifications. Moreover, it allows to fulfill the emission limits legislation. In this context, studies on the blends of diesel and propane fuels are poor in literature. Before using them in the engine, some preliminary investigations are necessary to know which are the effects of this mixed fuel in conventional injection systems. In this work, commercial diesel fuel and propane/diesel blends have been tested. In particular, two concentrations: 80% diesel and 20% propane, and 60% diesel and 40% propane have been prepared and stored in a pressurized tank. A conventional common rail injection system and a solenoid multi-hole injector have been used to deliver the fuel at high-pressure in a vessel at ambient temperature and pressure. Injection strategies in terms of energizing time and injection pressure have been taken from the functioning map of a real engine. Imaging measurements were focused on the near-nozzle field as the high volatility of the propane affects the spray behavior immediately after exiting from the injector nozzle. High-speed imaging has been performed using a long-distance microscopic objective and a synchronized flash-lamp. Measurements of the spray cone angle at the nozzle hole exit have been performed during the injection process. The tests showed that the propane/diesel blends have a wider angle than diesel. It is due to the high volatility of the propane more than on the injection pressure. To evaluate the effect of the operating condition and of propane concentration on the cone angle, the experimental results have been used to set-up an empirically derived correlation. It allowed to correlate the behavior of the cone angle of blended fuels to the case of pure diesel in the near-nozzle field.

Keywords

Propane/diesel blends, Spray cone angle, Near-nozzle field, High-speed imaging, Theoretical correlation.

Introduction

Compression ignition engines are widely used for transport and energy generation thanks to their high efficiency and low fuel consumption. Conversely, they are a source of pollutant emissions at the exhaust and they are strictly regulated. To face this issue, alternative combustion strategies than conventional diesel combustion have been recently proposed. Among these, low-temperature combustion (LTC) concepts are employed to limit the exhaust emissions while saving the engine efficiency. The main peculiarity of the LTC strategies is the improvement of the air-fuel mixing process by retarding the start of combustion. Use of fuels with high resistance to auto-ignition has proved attractive to this purpose. Therefore, blends of low and high reactivity fuels are used in the engine to control the reactivity of the charge. Many studies on LTC focused on the properties of the fuel injected in the intake manifold [1, 2, 3]; however, also the characteristics of the direct-injected fuel play a main role in the combustion process, as Benajes et al. [4] demonstrated. They studied the influence of the direct-injected fuel properties in a diesel engine running a reactivity controlled compression ignition combustion mode. Reijnders [5] investigated the efficacy of gasoline as a potential gas-to-liquid (GTL) Cetane Number suppressant in various dosages, in a compression ignition engine. Because of the increasing availability of lower Cetane Number fuels, Agarwal et al. [6] performed endoscopic visualization of the engine combustion chamber using diesel/kerosene and diesel/gasoline blends, that represent relatively inferior quality diesel fuels. While the influence on the exhaust and acoustic emissions of a diesel engine fed with different blends of short-chain alcohols/diesel fuel was investigated by Pinzi et al. [7]. These fuels were also studied by Huang et al. [8] that developed a new reduced diesel/natural gas mechanism for dual-fuel engine combustion and emission prediction; here, a mixture of methane, ethane, and propane was used to model the natural gas. Blending propane with diesel seems a good solution because of its low auto-ignition attitude and its availability in the fuels supply chain. Propane/diesel blends in the engine were already studied in the past; Ma et al. [9] ran experiments with these blends using a mechanical direct injection system in a diesel engine; they noted better atomization of the spray due to different density, viscosity, and vapor pressure of propane compared to diesel. Qi et al. [10] modified a single cylinder diesel engine with a mechanical direct injection system to operate with preformed liquid blends of propane/diesel, with a different mass rate of propane. However, the aforementioned

works concerned injection systems that are no longer up-to-date (mechanical direct injection systems). Hence, to evaluate the potential of propane/diesel blends in modern engines, new investigations are needed, using high-pressure injection systems.

The present work is part of a preliminary analysis that concerned the injection of blends of propane and diesel fuels in a compression ignition engine using a commercial common rail injection system [11, 12]. Before injecting the blends directly in the cylinder, the functioning of the conventional common rail injection system and the commercial multi-hole injector, designed only for diesel fuel, were assessed by running tests in a vessel at ambient conditions. Pure diesel fuel and propane/diesel blends were tested with different concentrations in weight: 80% diesel and 20% propane (named: P20), and 60% diesel and 40% propane (P40). The measurements focused on the near-nozzle field of the injection to evaluate the effect of the high volatility of the propane on the spray immediately after exiting from the injector nozzle. The experimental measurements were used to set-up an empirical model to correlate the spray cone angles of the blends with different concentrations of propane to the ones of pure diesel.

Experimental apparatus

Ambient temperature and pressure test bench

In order to verify the functioning of the common rail injection system when the blends of propane and diesel are processed instead of only diesel, a new test bench is set-up. The injection is performed in a system at ambient temperature and pressure. The test bench consists of a cylinder of plexiglass with a diameter of 30 cm (Figure 1) closed on one side by a metal disk where the injector is placed. The cylinder design aims to facilitate the positioning of the camera in front of the injector. The test bench is equipped with a suction system that removes the fuel from the test rig, to protect the camera from being invested by the fuel and to improve the quality of the recorded images. Any residual vapors are recovered by an additional extraction system in the laboratory. A commercial solenoid driven injector with 7 holes has been used. The characteristics of the injector are reported in Table 1.

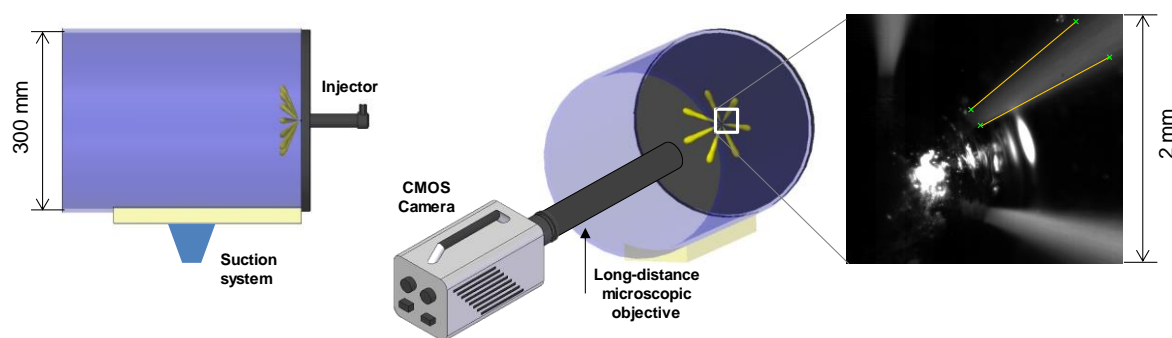


Figure 1. The test bench at ambient temperature and pressure.

Table 1. Injector specifications.

Injector type	Solenoid driven
Number of holes	7
Hole Diameter	0.141 mm
Injector holes angle	148°
Rated flow at 100bar	440 cm ³ /30s

Optical Setup

Digital imaging is performed by high-speed Complementary Metal-Oxide Semiconductor (CMOS) camera. The camera is the Photron FastCAM SA-X2, equipped with a long-distance microscopic objective. The region of interest is a portion of the injector tip (top-right sector), it is selected to ensure a good view of one spray. The height of the investigated area is 2 mm, as indicated in the image of Figure 1. 40000 frames per second are recorded, the exposure time is 24 μ s; this value gave the best compromise for a good temporal resolution and good luminosity of the image. The image height is 272 pixels, that correspond to a resolution of 136 pixels/mm. A ring flash, synchronized with the injection signal and with a power of 400W, is used to illuminate the spray during the injection process. The maximum duration of the flash is 3 ms.

Images have been processed in Matlab® environment using a home-made segmentation tool for the detection of the spray angle. Spray boundaries are found via background subtraction and edge detection methods. Then, the Hough transform is used to calculate the angles of the main lines detected in the image. Additional criteria have been implemented to take only the upper and lower profile of the selected jet. Finally, the cone angle is calculated as the difference between those of the upper and lower spray edges (yellow lines in Figure 1, left). The calculation is performed over 5 test repetitions.

Fuels properties and preparation

In table 2 the specific properties of diesel fuel, propane fuel, and fuel blends are reported. The properties of P20 and P40 have been obtained by linear interpolation [10] starting from the known properties of the diesel fuel and propane because of the unavailability of scientific data in the literature about the physical and chemical properties of the blends. Note that both the initial and final boiling points (IBP and FBP) correspond to a temperature below 0°C. Hence, propane is a gas at ambient conditions. For this reason, the blends have been prepared and stored in a tank under pressure with a capacity of 1.5 liters. The pressure in the return line of the injector has been kept greater than the saturation pressure of the propane at the ambient temperature (about 7-8 bar). Moreover, two valves, one on the supply and one on the return lines of the high-pressure pump, have been installed to keep the whole circuit under pressure and, then, to avoid the evaporation of the propane portion in the first stages of operation.

Table 2. Physical and chemical properties of the investigated fuels [13, 14].

Feature/Method	Units	Diesel	Diesel wt. 80% Propane wt. 20% (P20)	Diesel wt. 60% Propane wt. 40% (P40)	Propane C ₃ H ₈
Density at 15°C	[kg/m ³]	829	765	700	Liq. 508 Gas. 2
Heat of evaporation at ambient pressure	[kJ/kg]	250	285.4	320.8	427
Dynamic Viscosity Liquid	[Pa·s]	2.1·10 ⁻³	-	-	11·10 ⁻⁶
Kinematic Viscosity Liquid	[mm ² /s]	3.14	2.55	1.97	0.217
Cetane Number	[-]	51.8	41	30.3	-2
Distillation (ASTM D445)	IBP [°C]	159	-	-	-42.4
	10% vol. [°C]	194	-	-	-42.4
	50% vol. [°C]	268	-	-	-42.4
	95% vol. [°C]	350	-	-	-42.4
	FBP [°C]	361	-	-	-42.4

Engine operating conditions

The injection strategies used for this investigation derive from the homologation cycle Worldwide harmonized Light vehicles Test Cycle. In particular, they are 4 operating conditions (OCs) with 4 different injection pressure and energizing time of the injector. While the original strategies consist of two events, a pilot and a main injection, only the main injection is analyzed in this work because it is the one with longer duration. Table 3 reports the parameters of the injection strategies.

Table 3. Injection parameters of the investigated operating conditions.

Operating Condition	Energizing time [μs]	Injection pressure [bar]
OC1	545	615
OC2	520	700
OC3	570	867
OC4	560	891

Results and discussion

The experimental investigation is carried out to evaluate the cone angle of diesel fuel and propane/diesel blends via optical diagnostics. Images of the injection process in the near-nozzle field have been recorded with high spatial and temporal resolution and analyzed.

Figures 2 and 3 report a sequence of images of the injection process in the near-nozzle field for the three tested fuels, diesel, P20, and P40 in the operating condition 1, with 615 bar of injection pressure and 545 μs of energizing time. The time 0 μs refers to the first images where fuel can be detected. As a reference, the previous images without injection are also reported (time = -25 μs). Figure 2 arrives until 50 μs; while, Figure 3 goes from 75 μs up to 150 μs. It can be seen that only a portion of the injector tip can be visualized using the long-distance objective, allowing a high spatial resolution of the spray. In the second column of Figure 2, time = 0 μs, the fuel starts to exit from the injector holes. Even if the sprays look similar for the three fuels, as the propane concentration in the blend

increases, the spray seems to be less thick (see P40 at 0 μs). The high volatility of the propane is supposed to strongly affect the fuel evaporation since the early injection. At 25 μs , the effect of the different fuel properties is more evident. The spray of diesel early assumes a conical shape. The spray of P20 shows a not yet completely defined shape, with a wide opening and thin trails of fuel due to the droplets coming out of the nozzle. The shape of the spray of P40 is the most spread one, it does not resemble a conical shape; on the contrary, it has the widest opening among all the fuels and a very blurred aspect. The image blurring could be due to the theoretical highest fuel velocity for P40 since it has the lowest density. At the time of 50 μs (last column of Figure 2), the diesel fuel still has a conical shape, while the P20 reaches a quite fully developed conical shape, with a cone angle wider than for diesel. On the other hand, P40 fuel has such a wide angle to produce interference among the sprays exiting from the adjacent nozzle holes, as indicated by the white dashed circle in Figure 2. Figure 3 shows the spray evolution in the instants following the early injection phase. For all the tested fuels, the sprays assume a more or less steady configuration.

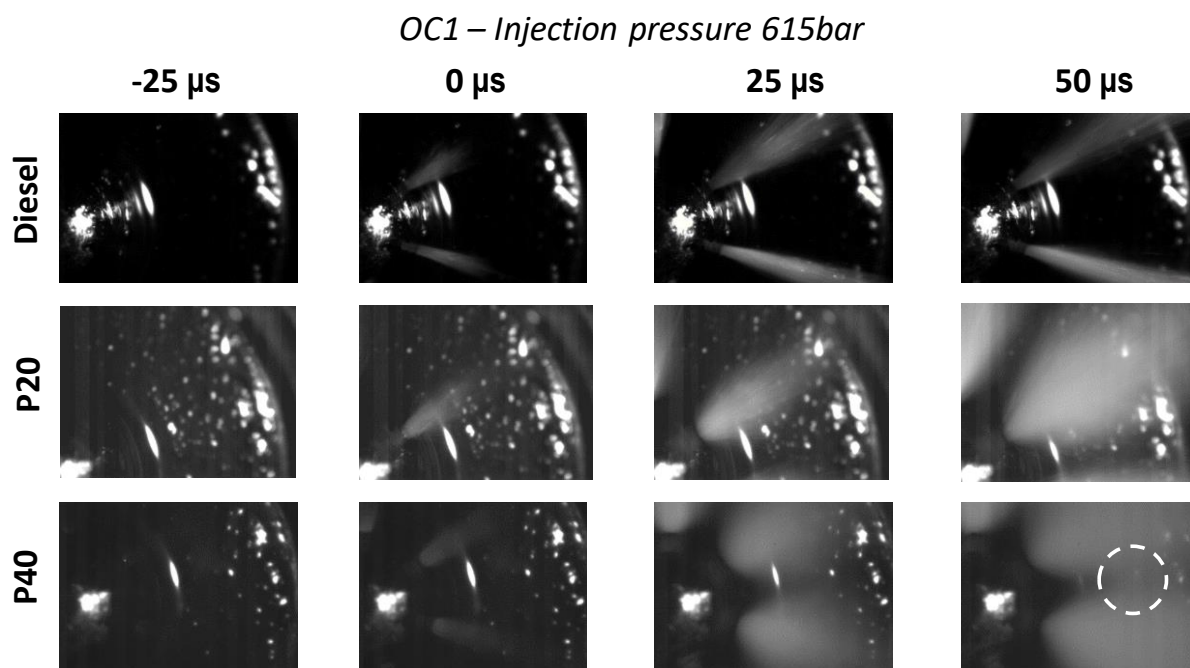


Figure 2. Images of injection process in the near-nozzle field for diesel, P20, and P40 fuels in the OC1, from 0 to 50 μs .

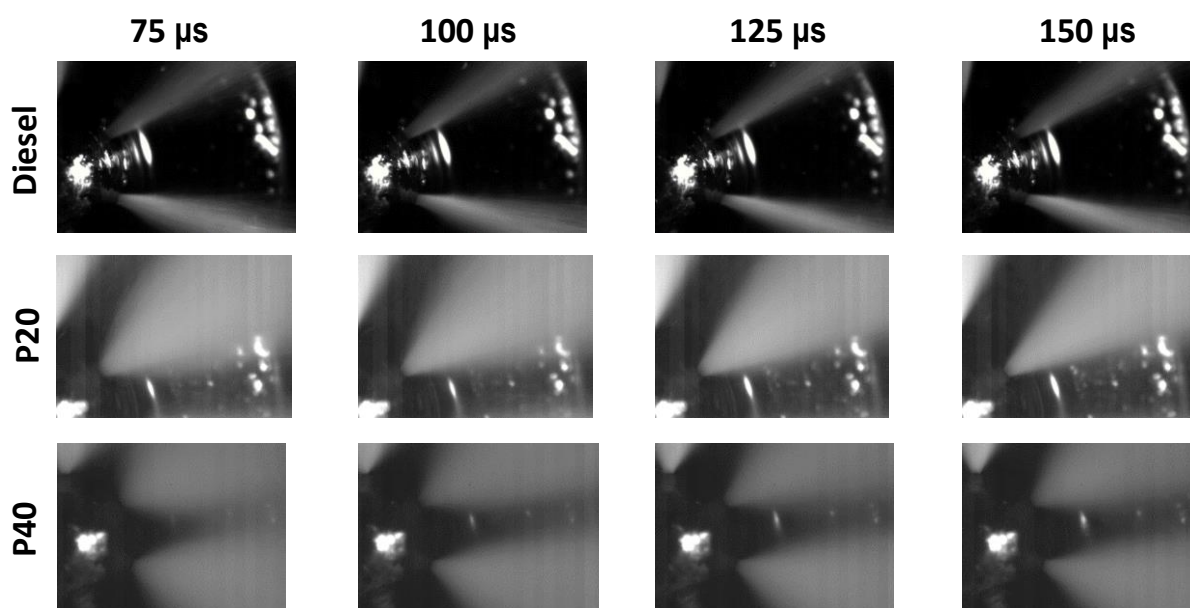


Figure 3. Images of injection process in the near-nozzle field for diesel, P20, and P40 fuels in the OC1, from 75 to 150 μs .

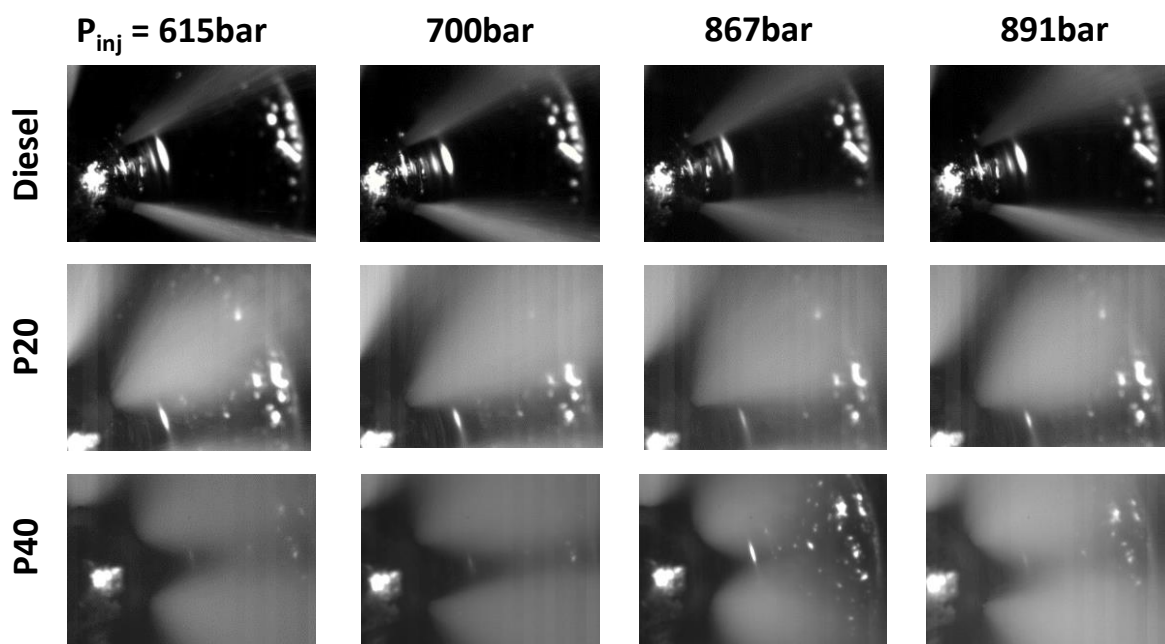


Figure 4. Images of injection process in the near-nozzle field for diesel, P20, and P40 fuels at 50 μ s with different injection pressure.

After 75 μ s, their shapes do not change much; they are characterized by smaller cone angles than the previous instants. This behavior is not clearly visible for the diesel, while it is more evident for the fuels P20 and P40. In particular, for P40, it seems that at 125 μ s there is no longer interference among the nearby sprays. In general, the angle of the stabilized spray is much wider for the propane/diesel blends than for the pure diesel. The time at 50 μ s seems to be where the spray approaches the steady condition. Figure 4 reports a selection of images at this time, for all the tested injection pressures and fuels. The pressure of injection is linked to the fuel velocity at the nozzle exit and it affects the atomization process [15]. Using the Bernoulli equation [16] and assuming the flow through the nozzle is quasi-steady, incompressible, and one dimensional, it is possible to calculate the injection velocity. It increases by 20%, for all the fuels, if the injection pressure rises from 615 bar (OC1) to 891 bar (OC4). Then better atomization and fuel dispersion are expected from OC1 to OC4. On the contrary, the images of Figure 4 do not show significant differences. The spray shape seems to preserve the same aspect for all the tested cases, keeping the previously discussed differences of the cone angles between the three fuels. The spray angle seems to be related more to the fuel properties than to the operating conditions, and an increment of injection pressure with atmospheric backpressure does not seem to affect the spray shape.

To better investigate this process, the spray cone angle has been measured for each condition. The evolution of spray cone angle versus time is reported in Figure 5, for all the tested fuels and OCs. In all the graphs, the upper region in gray represents angles higher than 51,4°, that is the angle between two adjacent nozzle holes. If the cone angle is higher than this value, there is interference among the sprays. It can be observed that for all the tested conditions, the propane/diesel blends always exceed that value, in turn in the early and in the late injection phase. The evolution of the cone angle versus time shows a repeatable, systematic behavior of the propane/diesel blends compared to the diesel fuel. As seen also in the images, the diesel assumes quite soon a conical shape that will keep for all the injection process, with some oscillations up to the end of injection. Concerning the propane/diesel blends, the visualization in the near-nozzle field allows to identify a variable behavior, depending on the injection phase. As the fuel exits from the nozzle hole, the propane portion finds the conditions of pressure and temperature good for the vaporization. The spray is opened by the propane fuel, whose specific volume is increasing. As the injection continues, the fresh injected fuel pushes forward the previously injected one; hence, the location of propane vaporization moves downstream, far from the nozzle. In this phase, from 75 μ s to about 400 μ s, with small differences among the OCs, the sprays of the propane/diesel blends are characterized by a slow reduction of the angle. Finally, at the end of injection, because of the injection pressure lowering, less fuel is injected and the region of vaporization moves back again, up to the hole exit. At this moment, in a different way for the P20 and P40, the spray angle increases again. In particular, the angle for P40 starts to increase earlier than for P20, as if the recession of the vaporization region is faster. This phenomenon could be due to the higher vaporization intensity and injection velocity of P40 fuel because of its higher percentage of propane. For all the tested injection pressures, the cone angle of the P40 is higher than P20. This is ascribed to the higher propane content that, during the evaporation, promotes the opening of the spray.

As stated earlier, the analysis of the cone angle of these two propane/diesel blends aims to understand if there is evidence of interference among adjacent sprays, since it can affect the combustion efficiency. The test performed at atmospheric conditions can be a starting point to assess the effect of the propane concentration on the spray cone angle. Then, these observations can be transferred to more detailed tests inside the engine where many data with reference diesel fuel are available.

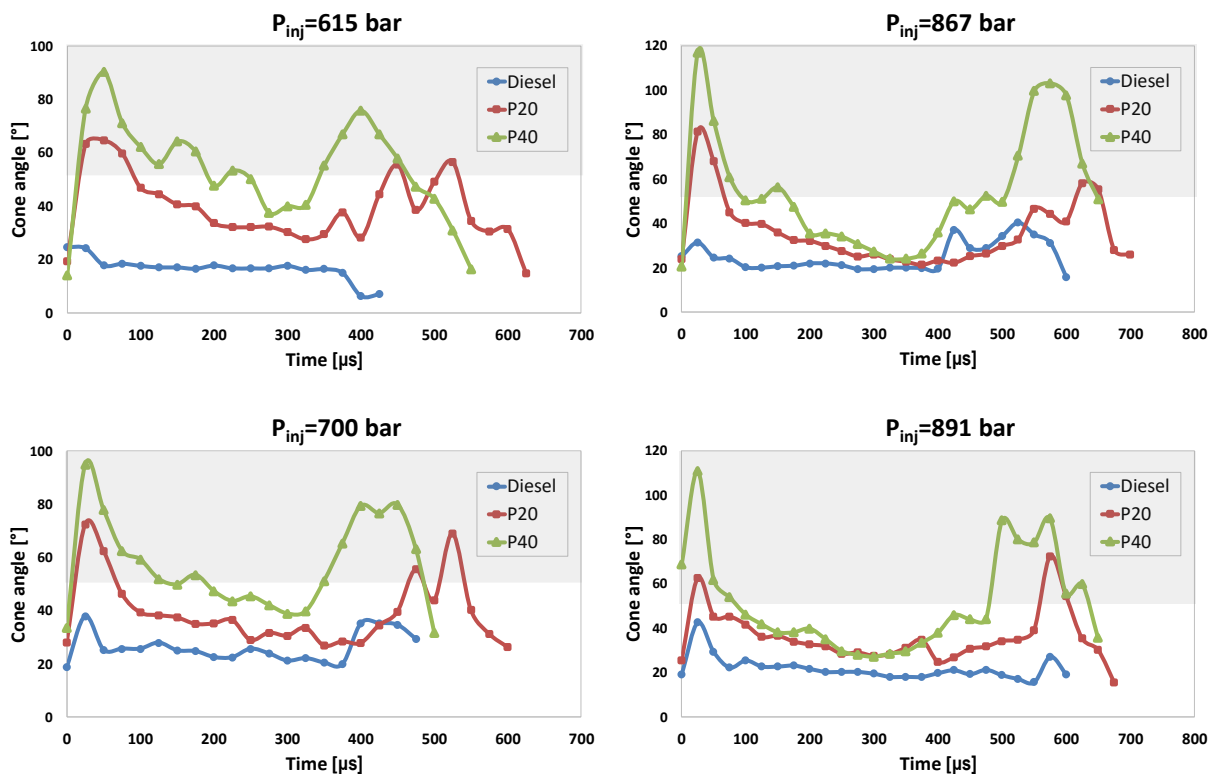


Figure 5. Measurements of cone angle in the near-nozzle field for diesel, P20, and P40 fuels for all the tested operating conditions.

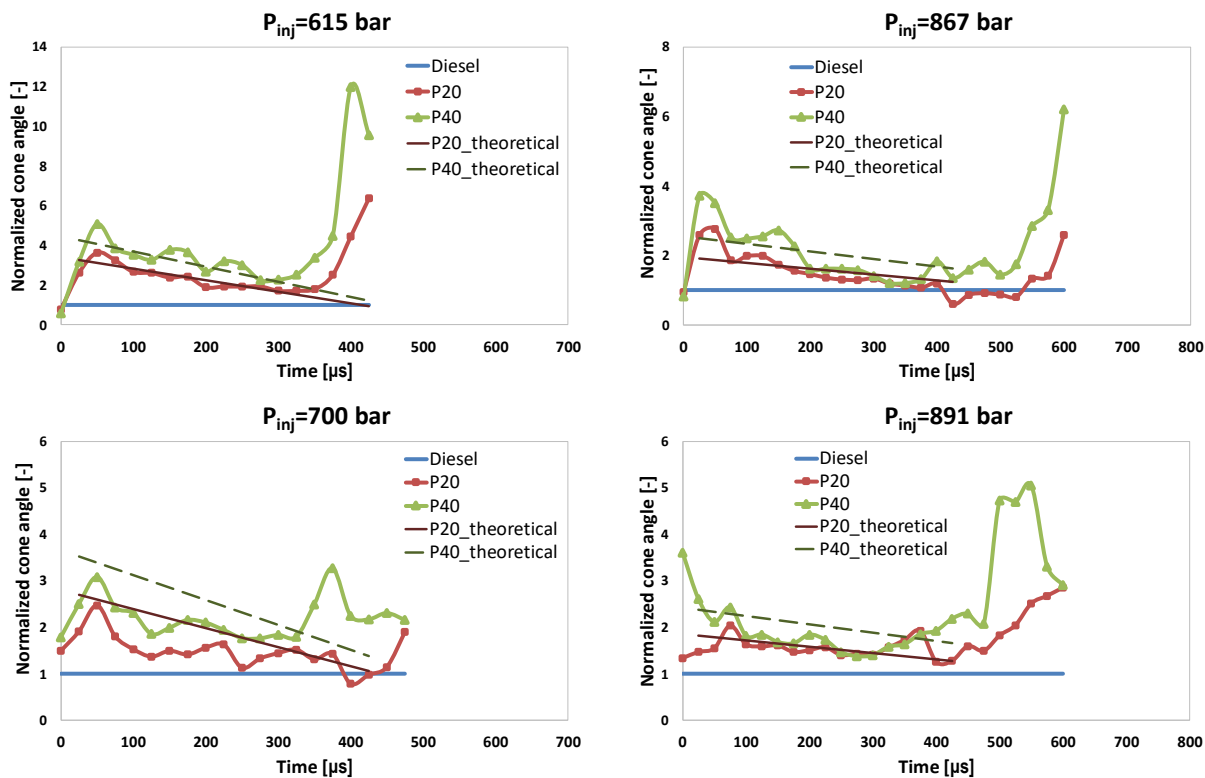


Figure 6. Normalized cone angles in the near-nozzle field with respect to diesel, for all the tested fuels and operating conditions.

The simplest way to evaluate the behavior of one fuel compared to another is to normalize the measurements on the reference fuel data. To this aim, the curves of cone angle versus time of P20 and P40, shown in Figure 5, have been normalized to the ones of diesel, for each OC. The normalized curves of cone angle are reported in Figure 6, up to the last available data of diesel fuel. In Figure 6, the curve relative to diesel is a constant line with value 1. In general, the normalized curve of P20 and P40 have a recurrent behavior; excluding the first measurement, they show an almost linear reduction up to a time that could be identified between 300 μ s and 400 μ s for all the OCs. Then, they have a sharp increment in almost all the cases, except for the injection pressure of 700 bar. This can be due to the normalization procedure that quits if diesel data is not available. The curves of Figure 6 also show an almost constant correlation between P20 and P40. In fact, dividing the curves of P40 to the corresponding ones of P20, the most frequent value of the ratio is in the range 1.2 - 1.3.

To verify the presence of a correlation between the operating conditions (injection pressure), fuel properties, and cone angle values, a theoretical model has been set-up using the normalized curves of Figure 6. First, the decreasing branch of each curve, from 25 μ s to 400 μ s, has been approximated with a linear correlation. Then, a scaling law between the lines of P20 and P40 was found, depending on the fuel density. Subsequently, using the lines of P20 for the various OCs, the slopes and the constant terms have been put in relation to the injection pressure. Finally, the following empirically derived correlation between the cone angle of the generic propane/diesel blend ($\vartheta_{P\%}$) and the one of diesel (ϑ_{diesel}) has been found versus time (t) :

$$\frac{\vartheta_{P\%}}{\vartheta_{diesel}} = 0.79 \left(\frac{\rho_{diesel}}{\rho_{P\%}} \right)^3 \cdot \left[\left(\frac{P_{amb}}{P_{inj}} \right) \cdot (-8.8t + 3070) + (0.0085t - 1.6) \right]; \quad \text{with } t \in [25, 400] \quad (1)$$

Where ρ_{diesel} is the density of diesel, $\rho_{P\%}$ is the density of the generic propane/diesel blend, P_{amb} is the backpressure, and P_{inj} is the injection pressure. As specified, this correlation is valid in the time range between 25 μ s and 400 μ s.

In Figure 6, the linear correlations obtained using eq.1 have been reported in the corresponding graphs. They approximate well the data at 615 bar of injection pressure for both P20 and P40 fuels. Also for 867 bar, the average evolution of the cone angle versus time has been caught. For 891 bar, since the experimental curves almost overlap for the two propane concentrations, only one theoretical curve fits the data, the one for P20; while the one for P40 over-predicts the data because of the influence of the density term. Finally, both the correlations for 700 bar of injection pressure over-predict the experimental data. This result was expected because this condition showed a behavior out of the trend; in fact, it exhibits the lowest cone angles while having a middle value of injection pressure.

Conclusions

Commercial diesel fuel and two blends of propane and diesel fuels with 20% and 40% of propane concentration in weight have been tested in a conventional high-pressure common rail injection system with a solenoid multi-hole injector. High-speed imaging in the near-nozzle field has been performed using a long-distance objective; the fuels have been injected in a vessel at atmospheric conditions. This investigation aimed to evaluate the behavior of the spray cone angle of the propane/diesel blends compared to the diesel one.

The tests showed that the propane/diesel blends are characterized by a variable value of the cone angle in the near field that depends on the high volatility of the propane more than on the injection pressure.

Diesel has a more or less constant cone angle over time. Conversely, propane/diesel blends have a wide angle in the early phase, it assesses to a smaller value later and, then, it increases again at the end of injection because of the drop of injection pressure. As the propane content in the blend increases, the spray cone angle increases too. The cone angles of the blends P20 and P40 normalized to the diesel showed a repeatable behavior by decreasing, first, and then sharply increasing at the end of injection. During the decreasing phase, a theoretical correlation has been set-up to compare the cone angle of a generic propane/diesel blend to the one of diesel fuel.

Acknowledgments

The authors would thank Mr. Carlo Rossi, for the technical assistance in the engine testing, and Mr. Bruno Sgammatto, for the assessment of electronic devices.

Nomenclature

CMOS	Complementary Metal-Oxide Semiconductor
FBP	Final boiling point
GTL	Gas-To-Liquid
IBP	Initial boiling point
LTC	Low-Temperature Combustion

OC	Operating condition
P20	Propane/diesel blend with 20% in weight of propane
P40	Propane/diesel blend with 40% in weight of propane
P_{amb}	Ambient pressure [bar]
P_{inj}	Injection pressure [bar]

Greek symbols

ϑ_{diesel}	Cone angle of diesel fuel [°]
$\vartheta_{P\%}$	Cone angle of the generic propane/diesel blend [°]
ρ_{diesel}	Density of diesel fuel [kg/m ³]
$\rho_{P\%}$	Density of the generic propane/diesel blend [kg/m ³]

References

- [1] J. Benajes, S. Molina, A. Garcá, and J. Monsalve-Serrano, "Effects of low reactivity fuel characteristics and blending ratio on low load RCCI (reactivity controlled compression ignition) performance and emissions in a heavy-duty diesel engine," *Energy*, vol. 90, pp. 1261–1271, 2015.
- [2] Y. Li, M. Jia, Y. Chang, M. Xie, and R. D. Reitz, "Towards a comprehensive understanding of the influence of fuel properties on the combustion characteristics of a RCCI (reactivity controlled compression ignition) engine," *Energy*, vol. 99, pp. 69–82, 2016.
- [3] S. Ma, Z. Zheng, H. Liu, Q. Zhang, and M. Yao, "Experimental investigation of the effects of diesel injection strategy on gasoline/diesel dual-fuel combustion," *Applied Energy*, vol. 109, pp. 202–212, 2013.
- [4] J. Benajes, A. Garcá, J. Monsalve-Serrano, and D. Villalta, "Exploring the limits of the reactivity controlled compression ignition combustion concept in a light-duty diesel engine and the influence of the direct-injected fuel properties," *Energy conversion and management*, vol. 157, pp. 277–287, 2018.
- [5] J. Reijnders, M. Boot, B. Johansson, and P. de Goey, "GTL—gasoline as a potential CN suppressant for GTL," *Fuel*, vol. 222, pp. 278–286, 2018.
- [6] A. K. Agarwal, Y. Jiotode, and N. Sharma, "Endoscopic visualization of engine combustion chamber using diesoline, diesosene and mineral diesel for comparative spatial soot and temperature distributions," *Fuel*, vol. 241, pp. 901–913, 2019.
- [7] S. Pinzi, M. Redel-Macás, D. Leiva-Candia, J. Soriano, and M. Dorado, "Influence of ethanol/diesel fuel and propanol/diesel fuel blends over exhaust and noise emissions," *Energy Procedia*, vol. 142, pp. 849–854, 2017.
- [8] H. Huang, D. Lv, J. Zhu, Z. Zhu, Y. Chen, Y. Pan, and M. Pan, "Development of a new reduced diesel/natural gas mechanism for dual-fuel engine combustion and emission prediction," *Fuel*, vol. 236, pp. 30–42, 2019.
- [9] Z. Ma, Z. Huang, C. Li, X. Wang, and H. Miao, "Combustion and emission characteristics of a diesel engine fuelled with diesel–propane blends," *Fuel*, vol. 87, no. 8-9, pp. 1711–1717, 2008.
- [10] D. Qi, Y. Z. Bian, Z. Ma, and C. Zhang, "Combustion and exhaust emission characteristics of a compression ignition engine using liquefied petroleum gas-diesel blended fuel," *Energy Conversion and Management*, 2007.
- [11] E. Mancaruso, R. Marialto, L. Sequino, B. M. Vaglieco, and M. Cardone, "Investigation of the injection process in a research CR diesel engine using different blends of propane-diesel fuel," in *2015-24-2477*, 2015.
- [12] M. Cardone, E. Mancaruso, R. Marialto, L. Sequino, and B. M. Vaglieco, "Characterization of combustion and emissions of a propane-diesel blend in a research diesel engine," in *2016-01-0810*, 2016.
- [13] G. Kalghatgi, *Fuel/engine interactions*. SAE, 2014.
- [14] *I.P. Standards for Petroleum and its Products*, Institute of Petroleum Std.
- [15] C. Baumgarten, *Mixture formation in internal combustion engines*. Springer Science & Business Media, 2006.
- [16] J. B. Heywood *et al.*, *Internal combustion engine fundamentals*. McGraw-hill New York, 1988, vol. 930.